Saudi Pharmaceutical Journal 30 (2022) 726–734

Contents lists available at ScienceDirect

Saudi Pharmaceutical Journal

journal homepage: www.sciencedirect.com

Original article

Abemaciclib-loaded ethylcellulose based nanosponges for sustained cytotoxicity against MCF-7 and MDA-MB-231 human breast cancer cells lines

Md. Khalid Anwer [a], Farhat Fatima [a], Mohammed Muqtader Ahmed [a,*], Mohammed F. Aldawsari [a], Amer S. Alali [a], Mohd Abul Kalam [b], Aws Alshamsan [b], Musaed Alkholief [b], Abdul Malik [b,*], Alanazi Az [c], Ramadan Al-shdefat [d]

[a] Department of Pharmaceutics, College of Pharmacy, Prince Sattam Bin Abdulaziz University, P.O. Box 173, Al-Kharj 11942, Saudi Arabia
[b] Department of Pharmaceutics, College of Pharmacy, King Saud University, P.O. Box 2457, Riyadh 11451, Saudi Arabia
[c] Department of Pharmacology and Toxicology, College of Pharmacy, King Saud University, P.O. Box 2457, Riyadh 11451, Saudi Arabia
[d] Department of Pharmaceutical Sciences, Faculty of Pharmacy, Jadara University, Irbid, Jordan

ARTICLE INFO

Article history:
Received 1 November 2021
Accepted 4 March 2022
Available online 6 April 2022

Keywords:
Abemaciclib
Biocompatibility
Cytotoxicity
Ethylcellulose
Nanosponges

ABSTRACT

Abemaciclib (AC) is a novel, orally available drug molecule approved for the treatment of breast cancer. Due to its low bioavailability, its administration frequency is two to three times a day that can decrease patient compliance. Sustained release formulation are needed for prolong the action and to reduce the adverse effects. The aim of current study was to develop sustained release NSs of AC. Nanosponges (NSs) was prepared by emulsion-solvent diffusion method using ethyl-cellulose (EC) and Kolliphor P-188 (KP-188) as sustained-release polymer and surfactant, respectively. Effects of varying surfactant concentration and drug: polymer proportions on the particle size (PS), polydispersity index (PDI), zeta potential (ζP), entrapment efficiency (%EE), and drug loading (%DL) were investigated. The results of AC loaded NSs (ACN1-ACN5) exhibited PS (366.3–842.2 nm), PDI (0.448–0.853), ζP (−8.21 to −19.7 mV), %EE (48.45–79.36%) and %DL (7.69–19.17%), respectively. Moreover, ACN2 showed sustained release of Abemaciclib (77.12 ± 2.54%) in 24 h Higuchi matrix as best fit kinetics model. MTT assay signified ACN2 as potentials cytotoxic nanocarrier against MCF-7 and MDA-MB-231 human breast cancer cells. Further, ACN2 displayed drug release property without variation in the % release after exposing the product at 25 °C, 5 °C, and 45 °C storage conditions for six months. This investigation proved that the developed NSs would be an efficient carrier to sustain the release of AC in order to improve efficacy against breast cancer.

1. Introduction

Breast cancer (BC) is the one of the most frequent cancer in women and leading cause of cancer-related-death worldwide, 2.6 million women were diagnosed with BC accounting for about 685,000 mortality cases. BC has become the primary cause of the demise of approximately 30% of cancer people accounting for all cancer types (Ferlay et al. 2015). Globally, 21st century's (2021) mammogram data reflects 30%, one of four of newly diagnosed cancers in women is breast cancer. Combined chemotherapeutics approaches have significantly lowered the number of deaths, mostly in women diagnosed at early stages compared to mono-therapy. Still, the chances of recurrence are noticed due to the acquired pharmacological resistance (Dieci et al. 2013; Myers et al., 2015; Siegel et al., 2017; Aggarwal et al., 2021). Targeted chemotherapeutics shows inhibitory action against target site with minimum off-target effects differ that have gained a lot of considerations and interest (Hanahan and Weinberg, 2011).

Studies have shown that progression by the cell-cycle is firmly controlled in the mammalian cells through a cluster of cyclins proteins, which in order are paired with and activates the serine-

* Corresponding authors.
E-mail addresses: mo.ahmed@psau.edu.sa (M.M. Ahmed), amoinudeen@ksu.edu.sa (A. Malik).

Peer review under responsibility of King Saud University.

Production and hosting by Elsevier

https://doi.org/10.1016/j.jsps.2022.03.019
1319-0164/

threonine kinase (cyclin dependent kinases) (Barkat et al. 2020; Corona and Generali, 2018).

Apart from this, it has also been noticed that multiple molecular anomalies, particularly alterations in the overexpression of cyclin D1, resulted in the interruption of the cellular pathways in the breast cancer cell types, found in approximately 50–70% of patients (Cancer Genome Atlas, 2012; Peurala et al. 2013).

The researchers have reported about the therapeutic activity of flavopiridol (first generation CDK4 and CDK6 inhibitor), which undertook clinical trials. Due to lack of target selectivity, it exhibited unsatisfactory results, including toxicity and other adverse effects (Gallorini et al. 2012; Jessen et al. 2007). Flavopiridol showed less activity alone but when combined with docetaxel it enhaces the apoptosis (Fornier et al. 2007). Afterwards, dinaciclib (second generation of CDK inhibitor) was found to have higher selectivity, but was restricted due to severe toxicity levels when tested in Phase I and a Phase II clinical trials (Fornier et al. 2007; Mita et al. 2014; Nemunaitis et al. 2013). The next generation of CDK inhibitors had shown advantage of easy administration through oral route and also exhibited greater selectivity, particularly targeting both CDK4 and CDK6, as compared to others (Das et al. 2020a; Finn et al. 2009; Fry et al. 2004). In 2004, palbociclib (PD-0332991) was reported as the first CDK4/CDK6-specific inhibitor (Toogood et al. 2005). In the next era, Abemaciclib (LY-2835219) and ribociclib (LEE011) were developed as CDK4/CDK6-specific inhibitors (Gelbert et al. 2014; Rader et al. 2013; Tate et al. 2014), and numerous clinical trial studies have been reported against varying cancer types such as breast cancer, non–small-cell lung cancer and colon cancer. Further, FDA and other regulatory agencies have significantly approved its applications in the treatment of breast cancer (Asghar et al. 2015; Fernandes et al. 2018). The major mechanism behind the anticancer properties of these inhibitors is that they block the activity of both CDK4 and CDK6-cyclin D, which causes inhibition of Rb phosphorylation, which suppresses gene transcriptions related to G1/S transitions (Dickson, 2014).

The Eli Lilly and Company Research Laboratories firstly discovered and identified the potential anti-breast cancer activity of Abemaciclib (LY2835219), showing high selectivity towards the inhibition of CDK4/cyclin D1 complexes and CDK6/cyclin D1 (Gelbert et al. 2014). In another study the researchers reported the anticancer activity of AC as it promoted the cellular aging phenotypes in breast cancer cells, shown by the existence of noticeable hypermethylation and accretion of endogenic β-galactosidase (Tripathy et al. 2017). Abemaciclib (LY2835219), chemical structure depicted in Fig. 1, inhibited the ATP-binding site of CDK4 and CDK6, and was 14 times more effective against CDK4 as compared to CDK6 (Lallena et al. 2015). Tablet dosage form of AC is available as "Verzenio" in dose strength ranged from 50 to 200 mg.

Moreover, drug targeting to specific site limits their applications. In this respect, nanotechnology has played a significant role; nanocarriers efficiently deliver the drug to a specific location with higher loading capacity in a sustained manner. Current studies have directed towards the development of nanoporous structures such as NSs for the competent chemotherapeutic drug targeting

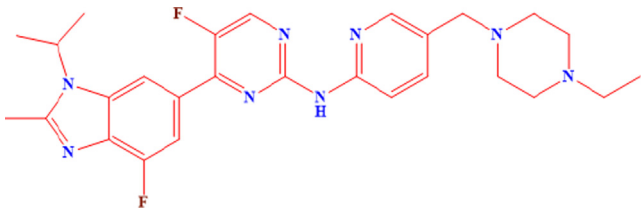

Fig. 1. Chemical structure of Abemaciclib.

(Das et al. 2020b; Sivasankarapillai et al. 2021). Nanosponges (NSs) possess a long length biodegradable polymers that promote the release of drug after polymer degradation. Polymers and cross linkers are the major excipients of NSs beside the drug. The nature of polymers determines the performance of drug loaded NSs. Various polymers like β-cyclodextrin, polyvinyl alcohol, ethyl cellulose, alginates, eudragit are used for the preparation of NSs. Cross linkers namely, dichloromethane, diphenyl carbonate, carboxylic acid dianhydride etc are used to link the polymer that results into formation of spherical pocket structure. These pockets can accommodate the drug (Prabhu et al. 2020). NSs have greater potential as safe, effective carriers for solubility enhancement of poorly soluble drugs due to tiny size, large porous surface area and high loading capacity (Trotta et al. 2012; Ahmed et al. 2020; Torne et al. 2013).

As per our findings, no study has been yet reported to sustained release and loading efficacy of AC-encapsulated ethyl-cellulose NSs. In this study, we prepared AC-loaded ethyl-cellulose NSs and optimized by particle characterization, drug loading and further evaluated for morphology, *in-vitro* release and cytotoxic study against MCF7 and MDA-MB-231 human breast carcinogenic cells.

2. Materials and methods

2.1. Materials

Abemaciclib (AC) was purchased from "Mesochem Technology" Beijing, China. Ethylcellulose (EC), dimethyl sulfoxide (DMSO), dichloromethane (DCM), Dulbecco's Modified Eagle's Medium (DMEM), and Fetal Bovine Serum (FBS) were obtained from "Sigma Aldrich, St. Louis, MO, USA". All other chemicals and solvents were used as received.

2.2. Fabrication of AC-encapsulated NSs

AC-encapsulated NSs (ACNs) were prepared by solvent emulsification-ultrasonication technique (Almutairy et al., 2021). NSs (NSs) of different compositions were developed using different proportions of ethyl cellulose (EC), and Koliphore P-188 (stabilizer; KP-188) as presented in Table 1. Drug-AC (50 mg) was dissolved in 1 mL DMSO, and EC was dissolved in 4 mL of DCM, separately and vortexed (IKA® VORTEX 3 vortex shaker, Staufen Germany) together for the complete dissolution of drug and polymer. This organic phase was then added dropwise into aqueous phase containing KP-188 and emulsified using probe sonication "(probe # 423, CL-18, Fisher scientific; USA)" at 65 % W for 5 min with 10-sec pulse on-off cycle. Drug-loaded dispersion system in a beaker was magnetically stirred at 700 rpm until the complete evaporation of organic solvent. Thereafter, the concentrated dispersion was centrifuged at 11,000 rpm for 15 min and washed with Milli-Q water (n = 3) to remove the adsorbed drug and free-dried "(Martin Christ Alpha-1-4LD freeze-drier, Osterode, Germany)" (Ahmed et al. 2020).

2.3. Characterization of Abemaciclib-encapsulated NSs

2.3.1. Particle size analysis

Mean particle size (PS), zeta potential (ζP), and polydispersity index (PDI) of all the prepared ACNs were analyzed using dynamic light scattering (Zetasizer Nano ZS instrument, Malvern Instruments, Worcestershire, UK) at room temperature (25 ± 3 °C). The samples were dispersed in Milli-Q water (1: 200) to form a monodisperse system and assessed in triplicates (Kalam et al, 2020).

Table 1
Formulation detail and particle characteristics of AC-loaded Nanosponges (ACNs).

NSs	Composition			Particle analysis (Mean ± SD, *n* = 3)			Encapsulation efficiency (%)	Drug loading (%)
	AC (mg)	EC (mg)	KP-188 (0.5%;mL)	PS (nm)	PDI	ZP (mV)		
ACN1	50	50	25	442.3 ± 2.34	0.770 ± 0.23	−14.64 ± 2.65	61.67 ± 2.54	2.12 ± 0.21
ACN2	50	100	25	366.3 ± 2.65	0.448 ± 0.34	−19.20 ± 4.08	79.36 ± 1.65	1.45 ± 0.32
ACN3	50	50	50	717.7 ± 3.56	0.519 ± 0.12	−13.65 ± 1.89	57.62 ± 1.32	2.83 ± 0.87
ACN4	50	100	50	547.9 ± 2.87	0.641 ± 0.23	−11.21 ± 1.12	48.45 ± 2.43	1.78 ± 0.34
ACN5	50	100	100	842.2 ± 4.65	0.853 ± 0.13	−8.21 ± 2.43	35.69 ± 2.87	1.79 ± 0.78

AC (Abemaciclib), EC (Ethyl Cellulose), KP-188 (Koliphor P-188), PS (Particle size), PDI (Polydispersity index), ZP (Zeta Potential) EE (Entrapment efficiency) and DL (Drug loading).

2.3.2. Entrapment efficiency and drug loading

Percent drug entrapment efficiency (%EE) and drug loading (% DL) of all prepared NSs (ACN1-ACN5) were estimated by indirect method (Khuroo et al., 2014; Anwer et al, 2019). The freshly prepared colloidal dispersion was centrifuged at 11,000 rpm, filtered through syringe filters of pore size 0.45 µm and analyzed by UV-spectrophotometer (Jasco Spectrophotometer V-630, Tokyo, Japan) at 296 nm wavelength. The %EE and %DL were estimated using the following equations (***Eq. (1) and (2)***):

$$\%EE = \frac{Amount\ of\ drug\ added\ (mg) - Amount\ of\ drug\ in\ supernatant\ (mg)}{Total\ amount\ of\ drug\ added\ (mg)} \times 100 \cdots \quad (1)$$

$$\%DL = \frac{Amount\ of\ drug\ added\ (mg) - Amount\ of\ drug\ in\ supernatant\ (mg)}{Total\ weight\ of\ freez\ dried\ nanosponges\ (mg)} \times 100 \cdots \quad (2)$$

2.3.3. Fourier-transform infrared spectroscopy (FTIR)

The possible drug-polymer chemical interactions, Ethyl cellulose (EC) and AC were examined by FTIR. Initially, a blank sample of potassium bromide (KBr) was run to eliminate the background errors. Further, pure AC and optimized (ACN2) were mixed separately with KBr, compressed by hydraulic press to form transparent discs. Spectra were recorded and analyzed within the wave number range of 4000–400 cm^{-1} using FTIR spectrophotometer (Jasco 4600 Mid-IR FTIR spectrometer, Tokyo, Japan).

2.3.4. Differential scanning calorimetry (DSC) studies

Differential Scanning Calorimetry (DSC) studies were performed to investigate the thermal behavior, melting, crystallization, and solid-to-solid transition of drug-excipients. Around 5 mg of pure AC and optimized ACN2 was crimped separately in aluminum pans and the empty aluminum pan was used as reference. Thereafter, the sealed pans were exposed for heating at a rate of 10 °C/min within a temperature range of 30–250 °C under inert nitrogen environment. (DSC N-650; Scinco, Seoul, Korea).

2.3.5. X-ray powder diffraction (XRD) studies

The XRD analysis was used to study the nature of the materials as crystalline or amorphous. Pure AC and optimized ACN2 were evaluated to study the XRD patterns of AC and its nature in the porous nanocarrier (ACN2). The XRD diffractograms were recorded from 5 to 60° in a 2θ scale using "Rigaku Ultima IV Diffractometer, Tokyo, Japan" operating at 35 kV, 15 mA with CuKα radiation.

2.3.6. Scanning electron microscopy (SEM)

Scanning Electron Microscopy (SEM) imaging was performed to represent the surface morphology of the drug and nanosponge. AC and optimized ACN2 was homogeneously spread separately over a clean metallic attached transparent two-sided adhesive slab and coated with conductive gold-metal in a thin film coater (Quorum Q150R S, East Sussex, UK) dried under vacuum. Morphological features of AC and ACN2 were scanned through SEM "(FEI QUANTA FEF 250, Tokyo, Japan)" focused electron beam over a surface to create an image. Image processing program was applied for surface morphology study.

2.4. In vitro diffusion study

In vitro drug diffusion study was executed to analyze the drug release behavior and kinetic mechanism of the optimized ACN2 NSs. Diffusion of pure drug (AC) and ACN2 was determined using dialysis membrane (MWCO: 14 kDa) method. Pure AC (10 mg) and its equivalent entrapped amount of NSs were dispersed in 5 mL of diffusion medium (phosphate buffer, pH 7.4), separately (Kalam et al, 2020). Then AC and ACN2 suspension were transferred into dialysis membrane tubing of regenerated cellulose (Pore size MD-25-14), tied on both the ends and immersed into 100 mL phosphate buffer (pH 7.4). The assembly was kept on a thermostatically controlled magnetic stirrer, maintained at physiological temperature 37 ± 1 °C and stirring at 50 rpm. At predetermined time intervals, 2 mL samples were withdrawn with replacement of same amount of freshly prepared diffusion medium to mimic the sink condition. The aliquots were analyzed at 296 nm in triplicate by UV–Vis Spectrophotometer "(Jasco UV/Visible Spectrophotometer V-630 Japan)" to plot cumulative release profile.

Moreover, the release mechanism of ACN2 was interpreted by fitting the drug release data into different mathematical models such as Zero order, First order, Higuchi-Matrix and Korsmeyer-Peppas kinetics using the following equations (***Eq. (3)***–(***6)***):

$$\text{For Zero order,} \quad C_t = C_0 + k_0 t \quad (3)$$

$$\text{For First order,} \quad \log C_t = \log C_0 - k_1 t / 2.303 \quad (4)$$

$$\text{For Higuchi} - \text{Matrix,} \quad C_t = kHkt_{\frac{1}{2}} \quad (5)$$

$$\text{For Korsmryer} - \text{Peppas,} \quad Mt/M\infty = Ktn \quad (6)$$

Fig. 2. Particle size and zeta potential of the optimized Abemaciclib-loaded Nanosponges (ACN2) (Mean ± SD, n = 3).

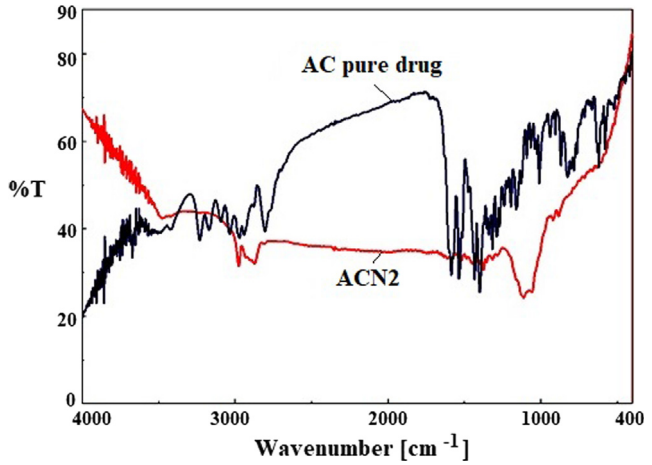

Fig. 3. Comparative FTIR spectra of pure AC and optimized Nanosponge (ACN2).

Where, C_t (Concentration of drug dissolved at time t), C_0 (Concentration of drug initially dissolved in the diffusion medium *i.e* zero), k_0 (zero-order rate constant), k_1 (first-order rate constant), $kH_{t1/2}$ (Higuchi matrix constant). M_t and M_∞ are cumulative release at time t and infinite time, respectively; k is a rate constant of ACN2 structural and geometric characteristics feature, t is the release time, and n denotes the diffusional exponent signifying the release mechanism. If n value is n < 0.5 (Quasi-Fickian diffusion), n = 0.5 (Fickian diffusion), 0.5 < n < 1.0 (anomalous (non-Fickian) diffusion, n = 1 (non-Fickian case-II), whereas, n > 1.0 represents (non-Fickian super case-II) release mechanisms.

2.5. Stability study

Stability studies of ACN2 was accomplished by transferring the sample into screw cap borosilicate (10 mL) laboratory reagent bottles making 3 sets each containing three samples. Each set was placed at three different temperature-conditions; RT (Room temperature; 25 ± 2 °C), FT (Freezing temperature; 4 ± 2 °C) and also AT (Accelerated thermal state; 60 ± 2 °C, 75% RH) (Saez et al., 2000; Abdelwahed et al., 2006). At predetermined time intervals (initially, 1st month, and 3rd month) samples were withdrawn and subjected to size, PDI, ZP, %EE, and %DR determination.

2.6. MTT assay

In vitro cytotoxicity of pure AC suspension and ACN2 against MCF-7 and MDA-MB-231 (human breast cancer cells) were performed using MTT (3-[4,5-dimethylthiazole-2-yl]-2,5-diphenylte trazolium bromide) assay. Initially, MCF7 and MDA-MB-231 carcinogenic cell lines were passaged in culture media composed of Dulbecco's Modified Eagle's Medium (DMEM) supplemented with the 10% Fetal Bovine Serum (FBS) incubated at 37 ± 1 °C in 5% CO_2 environment. Thereafter, 1 mL of cultured cell suspension ($\sim 5 \times 10^4$ cells/mL) was seeded into a 24-well plate and kept undisturbed in incubation for overnight. Samples under investigation was added separately into the pre-treated 96 well plates. Subsequently, 100 µL of MTT solution (5%, w/v) was added to the respective wells and again incubated at 37 °C for 4 h (Md et al, 2020). Further, the absorbance of each sample was measured at 490 nm using a ELISA microplate reader (Thermo Fisher Scientific, USA) and the % cell viability of was calculated by the following expression (***Eq. (7)***):

$$\%\text{Cell Viability} = \frac{\text{Mean absorbance of test sample}}{\text{Mean absorbance of control}} \times 100 \quad (7)$$

2.7. Statistical analysis

"The significance of difference between the means was determined by one-way analysis of variance (ANOVA) with post-hoc test. The p-value ($p < 0.05$) was considered as significant".

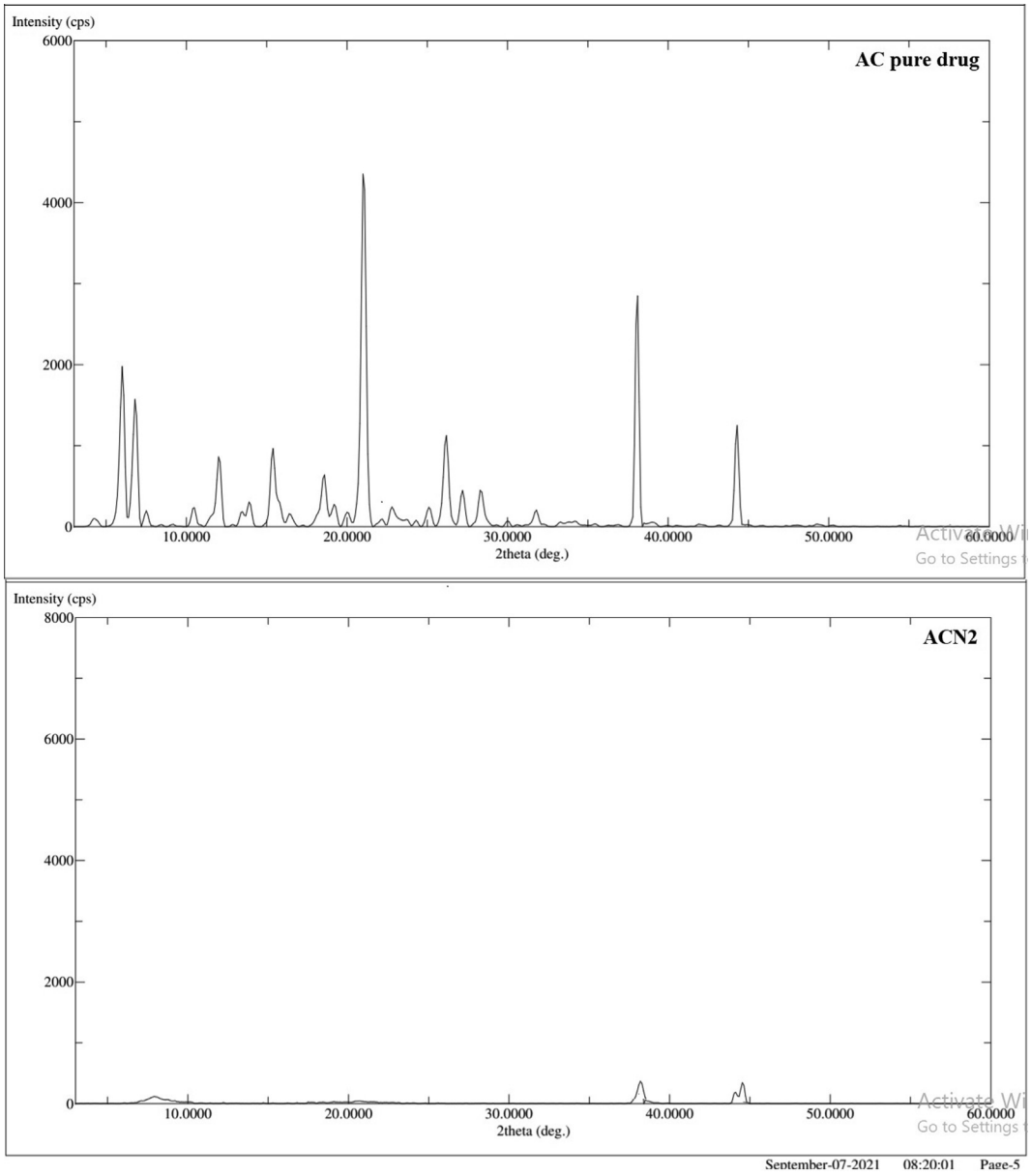

Fig. 5. The X-ray Diffractograms of pure AC (a) and the optimized Nanosponge (ACN2) (b).

3. Results and discussion

3.1. Evaluation of Abemaciclib-loaded NSs

In order to assess the effect of formulation composition on properties of five NSs with different content of EC, KP-188 were prepared (Table 1). The prepared NSs were evaluated for particle size, PDI, ZP, and percent drug encapsulation. The optimized formulae was further evaluated for morphology, *in vitro* release studies and *in vitro* MTT assay against breast cell lines.

3.2. Particle analysis

The prepared NSs exhibited particle size distribution within nano range (Table 1). It was observed that the NSs (ACN1-ACN5) showed particle size, PDI, and zeta potential in the range of 366.3–842.2 nm, 0.448–0.853, and −8.21 to −19.7 mV, respectively. The polymer (ethylcellulose) used in the formulation has a negative charge that assists in particle-particle repulsion, thus restricts particle agglomeration. The particle size increased from 442.3 to 717.7 nm with increase in volume of KP-188 (25–50 mL) in ACN1 and ACN3 formulae at AC: EC (1:1) ratio, respectively. Same trend also observed in formulae ACN2, ACN4 and ACN5 at AC: EC (1:2) ratio. ACN2 showed particle size (366.3 nm), PDI (0.448), in and zeta potential (−19.7 ± 0.157 mV) (Fig. 2), considered as optimized formulation. Large sized nanoparticles (>200 nm) usually reacts with interact with antigen presenting cells abundant on the tissues (Oh and Park, 2014).

3.3. Entrapment efficiency and drug loading calculations

The results of drug entrapment efficiency (%EE) and drug loading (%DL) of all the formulations have been illustrated in Table 1 and was found to be between 48.45–79.36% and 7.69 7–19.17%,

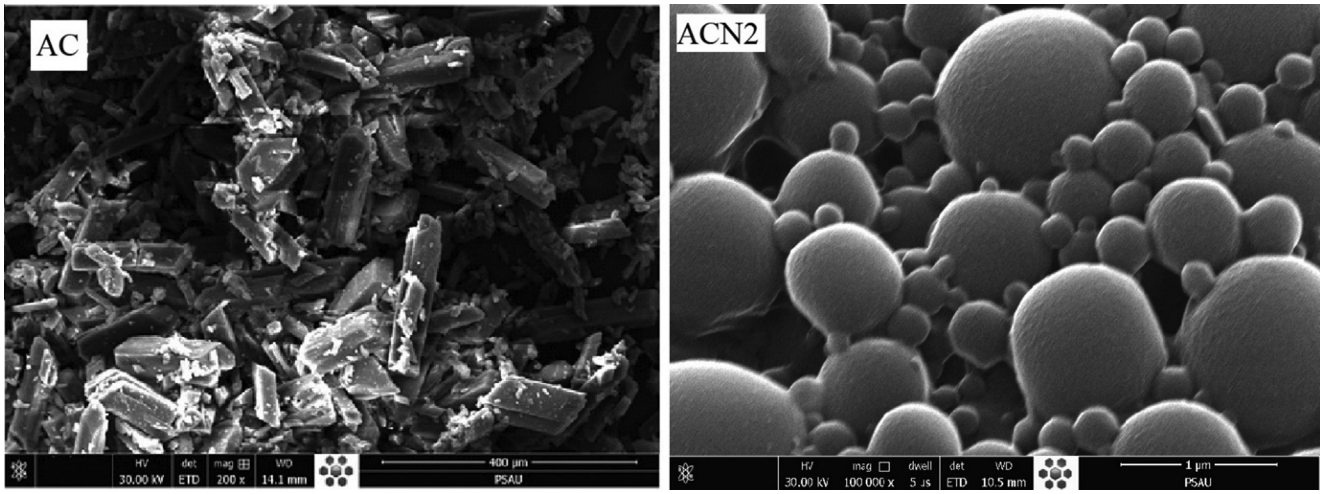

Fig. 6. SEM images for pure AC and the optimized Nanosponge (ACN2).

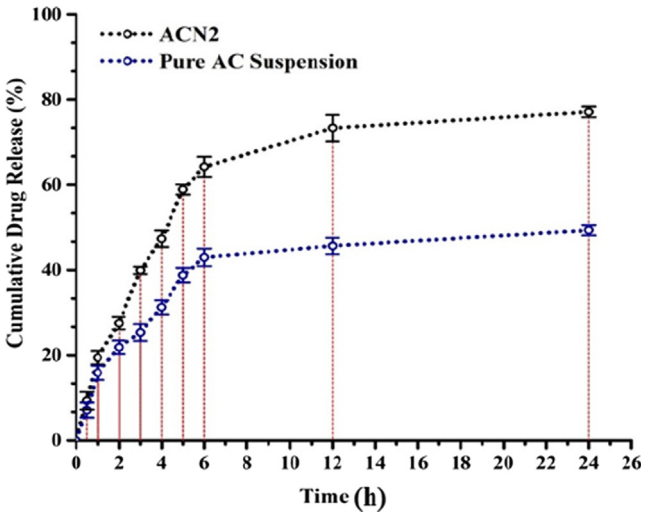

Fig. 7. Comparative *in vitro* release profile of pure AC and optimized ACN2 (Mean ± SD, n = 3).

respectively. Amongst all the ACNs, ACN2 exhibited most appropriate results of EE (79.36 ± 2.12%) and DL (19.17 ± 0.153%). The %EE increases from 61.67 to 79.36% with increase in content of EC (50–100 mg) at KP-188 (25 mL) in ACN1 and ACN2 formulae, respectively. But in the formula ACN3-ACN5, %EE decreased with increase in EC content and volume of KP-188. The highest %EE was detected. High encapsulation in ACN2 formula, probably due to presence of large amount of EC polymer and less amount KP-188 that prevents the leakage of drug from NSs (Sharma et al., 2016).

3.4. Fourier-transform infrared spectroscopy (FTIR)

FTIR spectra of pure drug and ACN2 are shown in Fig. 3. The few intense peak in the wavelength range of 1400–1600 cm^{-1} is attributed due to finger print region peaks. Results showed that the spectrum of ACN2 exhibited shifting of identical peaks of AC with the reduction in intensity in the fingerprint region of the drug (Monteiro & Airoldi, 1999; Padhi et al., 2016). This indicates that the drug was encapsulated within the polymer matrix.

3.5. Differential scanning calorimetry (DSC)

DSC is a useful tool for thermal behavior study, to assess whether drug particles have been entrapped in polymeric matrices (Anwer et al 2016). The DSC thermograms of pure AC and ACN2 are represented in Fig. 4. The thermogram of the pure AC has shown a two sharp endothermic peaks at 129.53 °C and 184.32 °C, and one exothermic peak at 140.61 °C, which was found closer to that reported in US patent (Albrecht and Rabe, 2017). However, thermogram of ACN2 does not exhibit any specific thermal peak of pure AC. This comparison clearly indicated that AC was completely encapsulated inside the spongy cavities of EC polymer matrix.

3.6. X-ray powder diffraction (XRD)

A comparative XRD spectra of pure drug AC and optimized Nanosponge (ACN2) are presented in Fig. 5. XRD diffractogram of pure drug exhibited various characteristic sharp and intense peaks at 6.00° (2θ), 6.80° (2θ), 12.00° (2θ), 15.40° (2θ), 18.60° (2θ), 21.00° (2θ), 26.2° (2θ), 38.10° (2θ)and 44.30° (2θ) as reported in literature, while, the number of peaks in ACN2 was found to be reduced. Thus, it indicated that the drug was adequately encapsulated within the

Table 2
Stability data of optimized Nanosponges (ACN2) (Mean ± SD, n = 3).

Storage condition	Months	Particle size (nm ± SD)	Zeta-potential (mV ± SD)	Encapsulation efficiency (%)	%DR (at 24 h)
–	0	366 ± 2.6	−19.2 ± 2.5	79.3 ± 1.6	77.1 ± 2.6
RT (25 ± 2 °C)	1	364 ± 1.4	−19.3 ± 1.9	77.5 ± 2.1	77.4 ± 2.3
	3	367 ± 6.3	−17.6 ± 3.1	76.1 ± 3.7	75.9 ± 2.9
FT (4 ± 2 °C)	1	363 ± 7.6	−18.8 ± 4.9	73.2 ± 1.9	72.5 ± 1.7
	3	374 ± 8.1	−16.7 ± 5.0	70.3 ± 1.5	71.2 ± 1.5
AT (60 ± 2 °C, 75% RH)	1	384 ± 9.6	−14.4 ± 2.3	66.7 ± 1.1	68.4 ± 2.0
	3	391 ± 7.5	−9.6 ± 1.7	61.4 ± 2.1	64.2 ± 1.2

RT = Room temperature; FT = Freezing temperature and AT = Accelerated temperature.

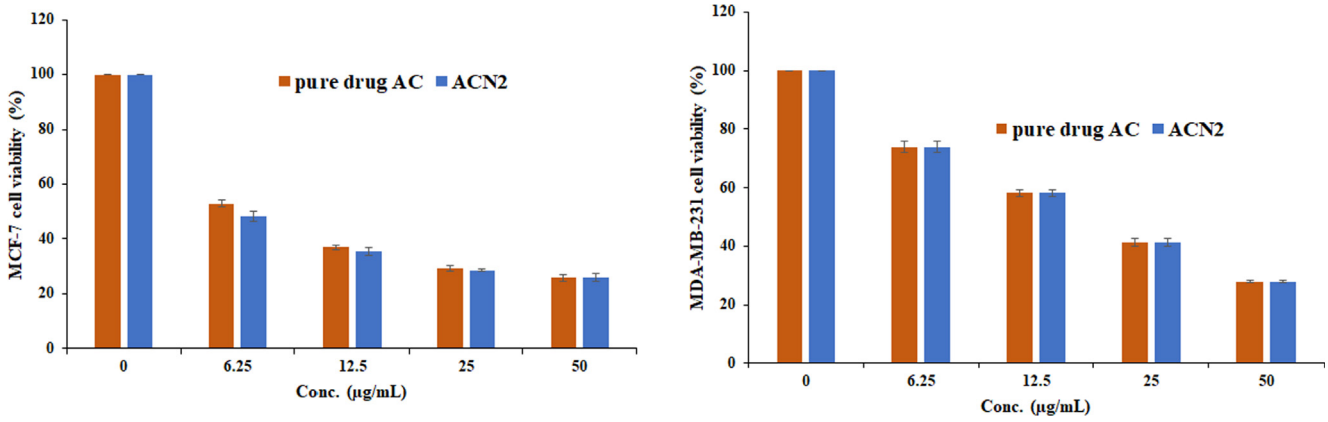

Fig. 8. MTT assay (cell viability) values of pure AC and optimized Nanosponge (ACN2).

polymer matrix in the Nanosponge. The crystallinity of pure drug was found to be reduced (as represented in Fig. 5), probably enhancing the amorphous behavior in ACN2. This clearly indicated transformation of crystalline to amorphous form due to the dispersion of drug AC into EC polymer sponge. The polymeric EC sponge covered drug, which prevent to come out at solid-air interface (Almutairy et al., 2021).

3.7. Scanning electron microscopy (SEM)

SEM micrographs of pure drug (AC) and the Nanosponge (ACN2) representing the crystallinity (Fig. 6), and spherical shape and smooth surface of Nanosponge with porous structure (Fig. 6), respectively. It could be advocated that the porous structure of ACN2 would be due to the in-ward diffusion of DCM on the EC (Almutairy et al., 2021). Due to the hydrophilicity, Kolliphore P-188 may leach out during the fabrication process, creating adherent over surface of porous nanosponge.

3.8. In-vitro diffusion study

This study assisted in determining the drug release behavior and the mechanism of drug release from the optimized Nanosponge (ACN2). As shown in Fig. 7, the drug release behavior showed an initial burst release within 4 h, followed by sustained-release up to 24 h (Al-nemrawi et al., 2022; Al-nemrawi et al., 2019). The optimized formulation (ACN2) and pure AC suspension showed a maximum drug release of around 77.12% and 49.33%, respectively, at 24 h. Furthermore, the results demonstrated that the release property of the drug from the NSs (ACN2) was enhanced as compared to pure drug suspension. The prolongation of drug release from the ACNs is possibly due to the slower dispersal of aqueous media within the hydrophobic polymer matrix. Presence of EC as a polymer exerted a significant role in regulating the release of AC from the matrix.

The release data of optimized NSs (ACN2) was fitted with different kinetic models to know the release mechanism. All the models showed varied regression coefficient (R^2) values, noted for zero-order (R^2 = 0.7421), first-order (R^2 = 0.7626) and Higuchi model (R^2 = 0.8675). The Higuchi model showed the highest R^2 value and thus was considered the best fit model for ACN2, implying sustained release behavior of AC from EC bilayer occurred as a result of AC diffusion through porous and swellable matrix diffusion from ACN2. Moreover, the Korsmeyer-Peppas model with diffusion-exponent ($0.45 < n < 0.89$) signified the non–Fickian release mechanism.

3.9. Stability study

No changes in physical appearance of the optimized Nanosponge (ACN2) was observed in all storage conditions throughout the study. After 3 months storage, optimized Nanosponge (ACN2) was found to be stable without any major changes in size, ZP, % EE and %DR (Table 2).

3.10. MTT assay

The MTT assay exhibited concentration dependent reduction in cell viability for pure drug and the optimized Nanosponge ACN2 against MCF-7 and MDA-MB-231 cell lines (Fig. 8). The IC_{50} values for pure drug AC and ACN2 were found 7.29 ± 0.25 and 6.00 ± 0. 34 µg/mL for MCF-7 cells and 18.58 ± 1.07 and 18.61 ± 0.36 µg/mL for MDA-MB-231, respectively. The ACN2 showed significant reduction in cell viability (48.14, 35.38, 28.59 and 26.03% at 6.25, 12.25. 25 and 50 µg/mL) in comparison to pure drug AC (52.85, 36.90, 29.32 and 25.76% at 6.25, 12.25. 25 and 50 µg/mL), respectively, against MCF-7 cells, however, ACN2 showed (69.32, 58.16, 42.10 and 23.85% at 6.25, 12.25. 25 and 50 µg/mL) in comparison to pure drug AC (73.92, 58.23, 41.36 and 27.92% at 6.25, 12.25. 25 and 50 µg/mL), respectively, against MDA-MB-231 cells. Based on the results of MTT assay, it was observed that ACN2 exhibited potential anticancer activity against breast cancer cell lines, probably due to enhance the release of drug from ACN2 in comparison to pure drug. AC loaded NSs could be used as potent carrier for the treatment of breast cancer.

4. Conclusion

In the current investigation, EC based nanosponges loaded with AC were developed and evaluated for particle characteristics. Solvent emulsification-ultrasonication technique was found suitable to prepare the NSs. By varying the proportions of EC (as sustained release polymer) and Kolliphor P-188 (as stabilizer), formulation was optimized. The optimized formulation (ACN2) exhibited an acceptable particle size, PDI, zeta potential, %EE and %DL values for its intended application. FTIR, DSC, XRD, and SEM studies revealed ACN2 was compatible with polymer without significant chemical interactions, the encapsulated drug was in amorphous state with spongy-smooth surface. Diffusion data of ACN2 showed that, after an initial burst effect of the drug release, the rate followed a sustained release phase. After 24 h of release studies, pure AC suspension and ACN2 exhibited around 49.33% and 77.12% of drug release respectively, where ACN2 followed Higuchi-Matrix model of release kinetics with asymmetrical non-Fickian release

mechanism. Conclusively, the NSs (ACN2) exhibited enhanced sustained release of AC and exerted a potential anticancer activity against both MCF-7 and MDA-MB-231 breast cancer cell lines. Thus, the developed formulation could be an excellent potential carrier for anti-cancer agent (AC) for the treatment of breast cancer.

Declaration of Competing Interest

The authors declare that they have no known competing financial interests or personal relationships that could have appeared to influence the work reported in this paper.

Acknowledgements

The authors extend their appreciation to King Saud University for funding this work through research supporting project (RSP-2021/376), Riyadh, Saudi Arabia.

References

Abdelwahed, W., Degobert, G., Fessi, H., 2006. Investigation of nanocapsules stabilization by amorphous excipients during freeze-drying and storage. Eur. J. Pharm. Biopharm. 63, 87–94.

Aggarwal, S., Verma, S.S., Aggarwal, S., Gupta, S.C., 2021. Drug repurposing for breast cancer therapy: Old weapon for new battle. Semin. Cancer Biol. 68, 8–20. https://doi.org/10.1016/j.semcancer.2019.09.012.

Ahmed, M.M., Fatima, F., Anwer, M.K., Ansari, M.J., Das, S.S., Alshahrani, S.M., 2020. Development and characterization of ethyl cellulose NSs for sustained release of brigatinib for the treatment of non-small cell lung cancer. J. Polym. Engn. 40, 823–832. https://doi.org/10.1515/polyeng-2019-0365.

Albrecht, W., Rabe, S., 2017. Abemaciclib form IV. Patent No. WO 2017/108781 Al.

Almutairy, B.K., Alshetaili, A., Alali, A.S., Ahmed, M.M., Anwer, M.K., Aboudzadeh, M. A., 2021. Design of Olmesartan Medoxomil-Loaded NSs for Hypertension and Lung Cancer Treatments. Polymers 13 (14), 2272. https://doi.org/10.3390/polym13142272.

Al-nemrawi, N.K., Alkhatib, R.Q., Ayyad, H., Alshraiedeh, N.A., 2022. Formulation and characterization of tobramycin-chitosan nanoparticles coated with zinc oxide nanoparticles. Saudi Pharm J. (in press). 10.1016/j.jsps.2022.01.016.

Al-Nemrawi, N.K., Alsharif, S., Alzoubi, K.H., Alkhatib, R.Q., 2019. Preparation and characterization of insulin chitosan-nanoparticles loaded in buccal films. Pharm. Dev. Technol. 24 (8), 967–974. https://doi.org/10.1080/10837450.2019.1619183.

Anwer, M.K., Al-Mansoor, M.A., Jamil, S., Al-Shdefat, R., Ansari, M.N., Shakeel, F., 2016. Development and evaluation of PLGA polymer based nanoparticles of quercetin. Int. J. Biol. Macromol. 92, 213–219.

Anwer, M.K., Ahmed, M.M., Ezzeldin, E., Fatima, F., Alalaiwe, A., Iqbal, M., 2019. Preparation of sustained release apremilast-loaded PLGA nanoparticles: in vitro characterization and in vivo pharmacokinetic study in rats. Int. J. Nanomed. 14, 1587–1595. https://doi.org/10.2147/IJN.S195048.

Asghar, U., Witkiewicz, A.K., Turner, N.C., Knudsen, E.S., 2015. The history and future of targeting cyclin-dependent kinases in cancer therapy. Nat. Rev. Drug. Discov. 14, 130–146. https://doi.org/10.1038/nrd4504.

Barkat, H.A., Das, S.S., Barkat, M.A., Beg, S., Hadi, H.A., 2020. Selective targeting of cancer signaling pathways with nanomedicines: challenges and progress. Future Oncol. 16, 2959–2979. https://doi.org/10.2217/fon-2020-0198.

Cancer Genome Atlas, N., 2012. Comprehensive molecular portraits of human breast tumours. Nature 490, 61–70. https://doi.org/10.1038/nature11412.

Corona, S.P., Generali, D., 2018. Abemaciclib: a CDK4/6 inhibitor for the treatment of HR+/HER2- advanced breast cancer. Drug Desg. Dev. Therapy 12, 321–330. https://doi.org/10.2147/DDDT.S137783.

Das, S.S., Alkahtani, S., Bharadwaj, P., Ansari, M.T., Mdf, A.L., Pang, Z., Hasnain, M.S., Nayak, A.K., Aminabhavi, T.M., 2020a. Molecular insights and novel approaches for targeting tumor metastasis. Int. J. Pharm. 585, 119556. https://doi.org/10.1016/j.ijpharm.2020.119556.

Das, S.S., Bharadwaj, P., Bilal, M., Barani, M., Rahdar, A., Taboada, P., Bungau, S., Kyzas, G.Z., 2020b. Stimuli-Responsive Polymeric Nanocarriers for Drug Delivery, Imaging, and Theragnosis. Polymers (Basel) 12. https://doi.org/10.3390/polym12061397.

Dickson, M.A., 2014. Molecular pathways: CDK4 inhibitors for cancer therapy. Clin. Cancer Res. 20, 3379–3383. https://doi.org/10.1158/1078-0432.CCR-13-1551.

Dieci, M.V., Arnedos, M., Delaloge, S., Andre, F., 2013. Quantification of residual risk of relapse in breast cancer patients optimally treated. Breast. 22 (Suppl 2), S92–S95. https://doi.org/10.1016/j.breast.2013.07.017.

Ferlay, J., Soerjomataram, I., Dikshit, R., Eser, S., Mathers, C., Rebelo, M., Parkin, D.M., Forman, D., Bray, F., 2015. Cancer incidence and mortality worldwide: sources, methods and major patterns in GLOBOCAN 2012. Int. J. Cancer. 136, E359–E386. https://doi.org/10.1002/ijc.29210.

Fernandes, M.T., Adashek, J.J., Barreto, C.M.N., Spinosa, A.C.B., de Souza Gutierres, B., Lopes, G., Del Giglio, A., Aguiar Jr., P.N., 2018. A paradigm shift for the treatment of hormone receptor-positive, human epidermal growth factor receptor 2-negative (HR+/HER2-) advanced breast cancer: a review of CDK inhibitors. Drugs Context. 7, 212555. https://doi.org/10.7573/dic.212555.

Finn, R.S., Dering, J., Conklin, D., Kalous, O., Cohen, D.J., Desai, A.J., Ginther, C., Atefi, M., Chen, I., Fowst, C., Los, G., Slamon, D.J., 2009. PD 0332991, a selective cyclin D kinase 4/6 inhibitor, preferentially inhibits proliferation of luminal estrogen receptor-positive human breast cancer cell lines in vitro. Breast Cancer Res. 11, R77. https://doi.org/10.1186/bcr2419.

Fornier, M.N., Rathkopf, D., Shah, M., Patil, S., O'Reilly, E., Tse, A.N., Hudis, C., Lefkowitz, R., Kelsen, D.P., Schwartz, G.K., 2007. Phase I dose-finding study of weekly docetaxel followed by flavopiridol for patients with advanced solid tumors. Clin Cancer Res. 13, 5841–5846. https://doi.org/10.1158/1078-0432.CCR-07-1218.

Fry, D.W., Harvey, P.J., Keller, P.R., Elliott, W.L., Meade, M., Trachet, E., Albassam, M., Zheng, X., Leopold, W.R., Pryer, N.K., Toogood, P.L., 2004. Specific inhibition of cyclin-dependent kinase 4/6 by PD 0332991 and associated anti-tumor activity in human tumor xenografts. Mol. Cancer. Ther. 3, 1427–1438.

Gallorini, M., Cataldi, A., di Giacomo, V., 2012. Cyclin-dependent kinase modulators and cancer therapy. BioDrugs. 26, 377–391. https://doi.org/10.1007/BF03261895.

Gelbert, L.M., Cai, S., Lin, X., Sanchez-Martinez, C., Del Prado, M., Lallena, M.J., Torres, R., Ajamie, R.T., Wishart, G.N., Flack, R.S., Neubauer, B.L., Young, J., Chan, E.M., Iversen, P., Cronier, D., Kreklau, E., de Dios, A., 2014. Preclinical characterization of the CDK4/6 inhibitor LY2835219: in-vivo cell cycle-dependent/independent anti-tumor activities alone/in combination with gemcitabine. Invest. New. Drugs. 32, 825–837. https://doi.org/10.1007/s10637-014-0120-7.

Hanahan, D., Weinberg, R.A., 2011. Hallmarks of cancer: the next generation. Cell 144, 646–674. https://doi.org/10.1016/j.cell.2011.02.013.

Jessen, B.A., Lee, L., Koudriakova, T., Haines, M., Lundgren, K., Price, S., Nonomiya, J., Lewis, C., Stevens, G.J., 2007. Peripheral white blood cell toxicity induced by broad spectrum cyclin-dependent kinase inhibitors. J. Appl. Toxicol. 27, 133–142. https://doi.org/10.1002/jat.1177.

Kalam, M.A., Alkholief, M., Badran, M., Alshememry, A., Alshamsan, A., 2020. Co-encapsulation of metformin hydrochloride and reserpine into flexible liposomes: Characterization and comparison of in vitro release profile. J. Drug. Deliv. Sci. Technol. 57, 101670. https://doi.org/10.1016/j.jddst.2020.101670.

Khuroo, T., Verma, D., Talegaonkar, S., Padhi, S., Panda, A.K., Iqbal, Z., 2014. Topotecan-tamoxifen duple PLGA polymeric nanoparticles: investigation of in vitro, in vivo and cellular uptake potential. Int. J. Pharm. 473, 384–394. https://doi.org/10.1016/j.ijpharm.2014.07.022.

Lallena, M.J., Boehnke, K., Torres, R., Hermoso, A., Amat, J., Calsina, B., De Dios, A., Buchanan, S., Du, J., Beckmann, R.P., Gong, X., McNulty, A., 2015. Abstract 3101: In-vitro characterization of Abemaciclib pharmacology in ER+ breast cancer cell lines. Mol. Cell. Biol., 3101

Md, S., Alhakamy, N.A., Aldawsari, H.M., Husain, M., Kotta, S., Abdullah, S.T., A. Fahmy, U., Alfaleh, M.A., Asfour, H.Z., 2020. Formulation Design, Statistical Optimization, and In Vitro Evaluation of a Naringenin Nanoemulsion to Enhance Apoptotic Activity in A549 Lung Cancer Cells. Pharmaceuticals 13, 152. 10.3390/ph13070152.

Mita, M.M., Joy, A.A., Mita, A., Sankhala, K., Jou, Y.M., Zhang, D., Statkevich, P., Zhu, Y., Yao, S.L., Small, K., Bannerji, R., Shapiro, C.L., 2014. Randomized phase II trial of the cyclin-dependent kinase inhibitor dinaciclib (MK-7965) versus capecitabine in patients with advanced breast cancer. Clin Breast Cancer. 14, 169–176. https://doi.org/10.1016/j.clbc.2013.10.016.

Monteiro Jr., O.A., Airoldi, C., 1999. Some studies of crosslinking chitosan-glutaraldehyde interaction in a homogeneous system. Int. J. Biol. Macrol. 26 (2–3), 119–128. https://doi.org/10.1016/s0141-8130(99)00068-9.

Myers, E.R., Moorman, P., Gierisch, J.M., Havrilesky, L.J., Grimm, L.J., Ghate, S., et al., 2015. Benefits and harms of breast cancer screening: a systematic review. JAMA 314, 1615–1634.

Nemunaitis, J.J., Small, K.A., Kirschmeier, P., Zhang, D., Zhu, Y., Jou, Y.M., Statkevich, P., Yao, S.L., Bannerji, R., 2013. A first-in-human, phase 1, dose-escalation study of dinaciclib, a novel cyclin-dependent kinase inhibitor, administered weekly in subjects with advanced malignancies. J. Transl. Med. 11, 259. https://doi.org/10.1186/1479-5876-11-259.

Oh, N., Park, J.H., 2014. Endocytosis and exocytosis of nanoparticles in mammalian cells. Int. J. Nanomed. 9 (Suppl 1), 51–63. https://doi.org/10.2147/ijn.s26592.

Padhi, S., Mirza, M.A., Verma, D., Khuroo, T., Panda, A.K., Talegaonkar, S., Khar, R.K., Iqbal, Z., 2016. Revisiting the nanoformulation design approach for effective delivery of topotecan in its stable form: an appraisal of its in vitro Behavior and tumor amelioration potential. Drug Delivery 23 (8), 2827–2837. https://doi.org/10.3109/10717544.2015.1105323.

Peurala, E., Koivunen, P., Haapasaari, K.M., Bloigu, R., Jukkola-Vuorinen, A., 2013. The prognostic significance and value of cyclin D1, CDK4 and p16 in human breast cancer. Breast Cancer Res. 15, R5. https://doi.org/10.1186/bcr3376.

Prabhu, P.P., Mehta, C.H., Nayak, U.Y., 2020. NSs-Revolutionary Approach: A Review. Res. J. Pharm. Tech. 13 (7), 3536–3544. https://doi.org/10.5958/0974-360X.2020.00626.5.

Rader, J., Russell, M.R., Hart, L.S., Nakazawa, M.S., Belcastro, L.T., Martinez, D., Li, Y., Carpenter, E.L., Attiyeh, E.F., Diskin, S.J., Kim, S., Parasuraman, S., Caponigro, G., Schnepp, R.W., Wood, A.C., Pawel, B., Cole, K.A., Maris, J.M., 2013. Dual CDK4/CDK6 inhibition induces cell-cycle arrest and senescence in neuroblastoma.

Clin. Cancer Res. 19, 6173–6182. https://doi.org/10.1158/1078-0432.CCR-13-1675.
Saez, A., Guzmán, M., Molpeceres, J., Aberturas, M.R., 2000. Freeze-drying of polycaprolactone and poly(-lactic-glycolic) nanoparticles induce minor particle size changes affecting the oral pharmacokinetics of loaded drugs. Eur. J. Pharm. Biopharm. 50, 379–387.
Sharma, N., Madan, P., Lin, S., 2016. Effect of process and formulation variables on the preparation of parenteral paclitaxel-loaded biodegradable polymeric nanoparticles: A co-surfactant study. Asian. J. Pharm. Sci. 11, 404–416. https://doi.org/10.1016/j.ajps.2015.09.004.
Siegel, R.L., Miller, K.D., Jemal, A., 2017. Cancer statistics, 2017. CA Cancer J. Clin. 67, 7–30.
Sivasankarapillai, V.S., Das, S.S., Sabir, F., Sundaramahalingam, M.A., Colmenares, J. C., Prasannakumar, S., Rajan, M., Rahdar, A., Kyzas, G.Z., 2021. Progress in natural polymer engineered biomaterials for transdermal drug delivery systems. Mater. Today Chem. 19. https://doi.org/10.1016/j.mtchem.2020.100382.
Tate, S.C., Cai, S., Ajamie, R.T., Burke, T., Beckmann, R.P., Chan, E.M., De Dios, A., Wishart, G.N., Gelbert, L.M., Cronier, D.M., 2014. Semi-mechanistic pharmacokinetic/pharmacodynamic modeling of the anti-tumor activity of LY2835219, a new cyclin-dependent kinase 4/6 inhibitor, in mice bearing human tumor xenografts. Clin. Cancer Res. 20, 3763–3774. https://doi.org/10.1158/1078-0432.CCR-13-2846.
Toogood, P.L., Harvey, P.J., Repine, J.T., Sheehan, D.J., VanderWel, S.N., Zhou, H., Keller, P.R., McNamara, D.J., Sherry, D., Zhu, T., Brodfuehrer, J., Choi, C., Barvian, M.R., Fry, D.W., 2005. Discovery of a potent and selective inhibitor of cyclin-dependent kinase 4/6. J. Med. Chem. 48, 2388–2406. https://doi.org/10.1021/jm049354h.
Torne, S., Darandale, S., Vavia, P., Trotta, F., Cavalli, R., 2013. Cyclodextrin-based NSs: effective nanocarrier for tamoxifen delivery. Pharm. Dev. Technol. 18, 619–625. https://doi.org/10.3109/10837450.2011.649855.
Tripathy, D., Bardia, A., Sellers, W.R., 2017. Ribociclib (LEE011): Mechanism of Action and Clinical Impact of This Selective Cyclin-Dependent Kinase 4/6 Inhibitor in Various Solid Tumors. Clin. Cancer Res. 23 (13), 3251–3262. https://doi.org/10.1158/1078-0432.CCR-16-3157.
Trotta, F., Zanetti, M., Cavalli, R., 2012. Cyclodextrin-based NSs as drug carriers. Beilstein J. Org. Chem. 8, 2091–2099. https://doi.org/10.3762/bjoc.8.235.